

Fig. 1. Schematic diagram of the manufacturing process. The left part shows the SLM process for fabricating a copper substrate, with a laser beam directed at a substrate to create a grid-like structure. The right part shows the CVD process for graphene growth on the SLM copper substrate, with CH₄ and H₂ gases in a tube reactor. The diagram is labeled "Copper substrate fabricated via SLM" and "Graphene growth on SLM copper via CVD".

3. Results and discussion

3.1. Formation of SLM copper

3.1.1. SLM manufacturing of copper under different line energy densities

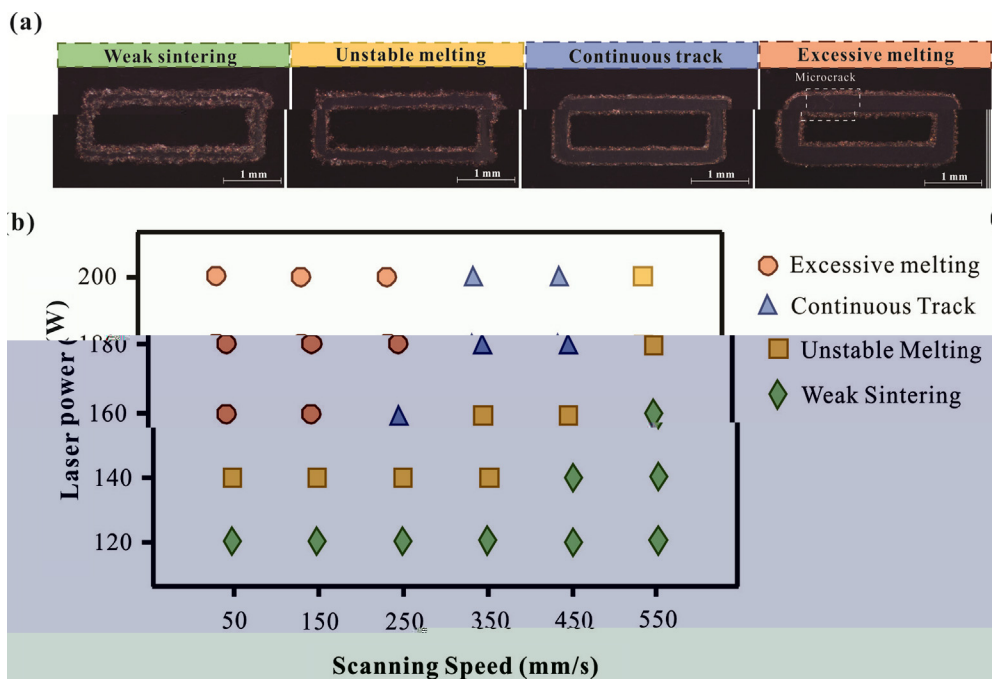


Fig. 2. SEM images of SLM copper tracks under different conditions: (a) Weak sintering, (b) Unstable melting, (c) Continuous track, and (d) Excessive melting. The figure shows four SEM images of rectangular tracks with 1 mm scale bars. The legend for (b) is: Excessive melting (orange circle), Continuous Track (blue triangle), Unstable Melting (brown square), Weak Sintering (green diamond).

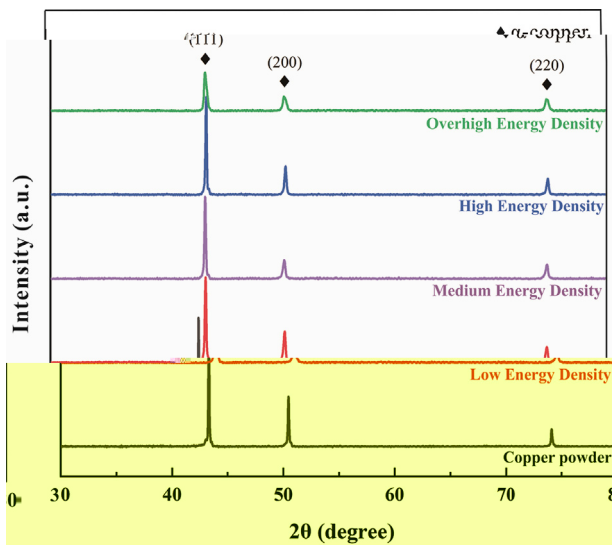


Fig. 3. RD

3.1.2. Formation of anisotropic microstructure under different volumetric energy density

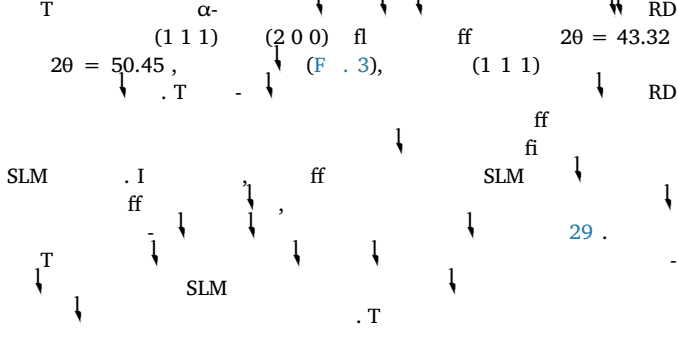
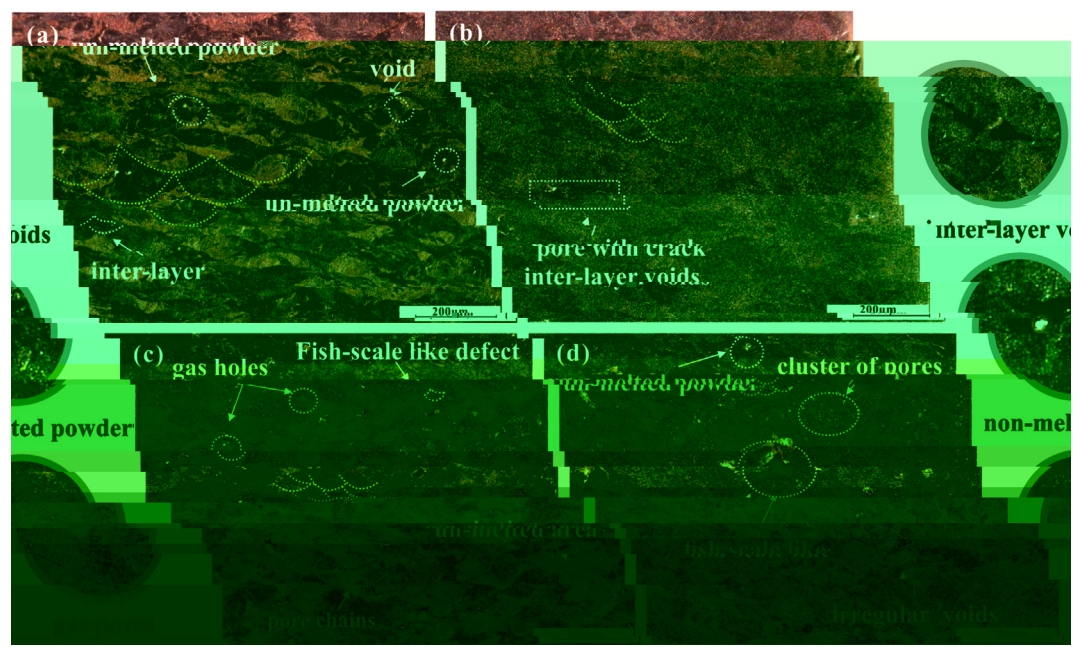


Fig. 4. O



(285 J/cm³), (128 J/cm³), (3000 J/cm³), (857 J/cm³)

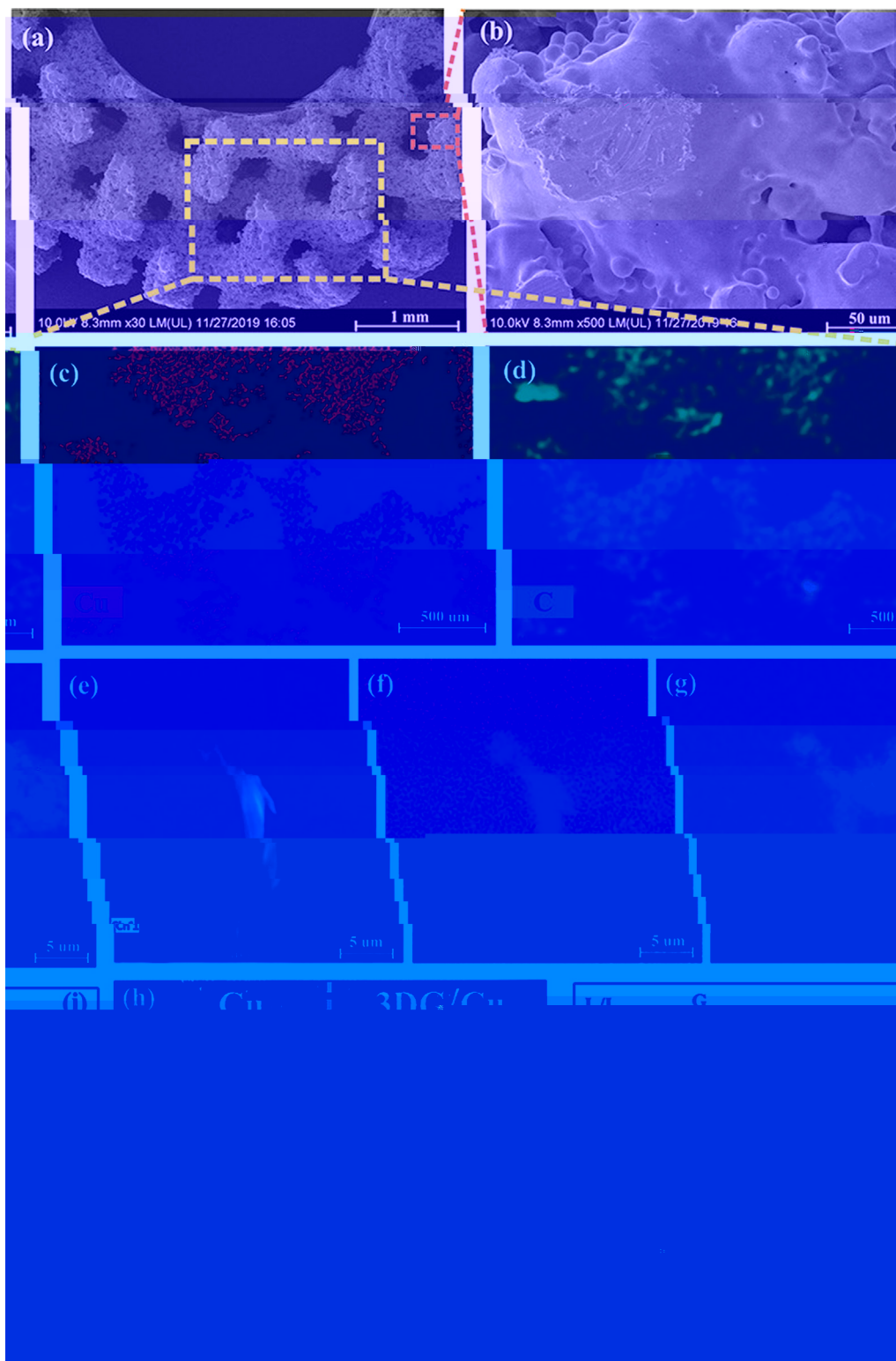


Fig. 8. (a) SEM image of the scaffold at 1 mm scale. (b) High-magnification SEM image of the porous structure at 50 μm scale. (c) EDS elemental map showing Carbon (C) in red. (d) EDS elemental map showing Oxygen (O) in green. (e), (f), and (g) are EDS line scans across the scaffold structure at 5 μm scale. (h) EDS line scan showing the presence of Copper (Cu) in the scaffold structure.

3.4. Thermal property and EMI shielding effectiveness of 3DG/Cu porous scaffolds

The thermal stability of the 3DG/Cu porous scaffolds was evaluated using TGA. The TGA curves show the weight loss of the scaffolds as a function of temperature. The 3DG/Cu porous scaffolds exhibit a weight loss of approximately 26.8% at 1000 °C, which is attributed to the decomposition of the 3DG component. The weight loss of the pure 3DG is approximately 14.8% at 1000 °C. The TGA curves of the 3DG/Cu porous scaffolds are shown in Fig. 9. The weight loss of the scaffolds is significantly higher than that of the pure 3DG, indicating that the scaffolds are more thermally stable than the pure 3DG.

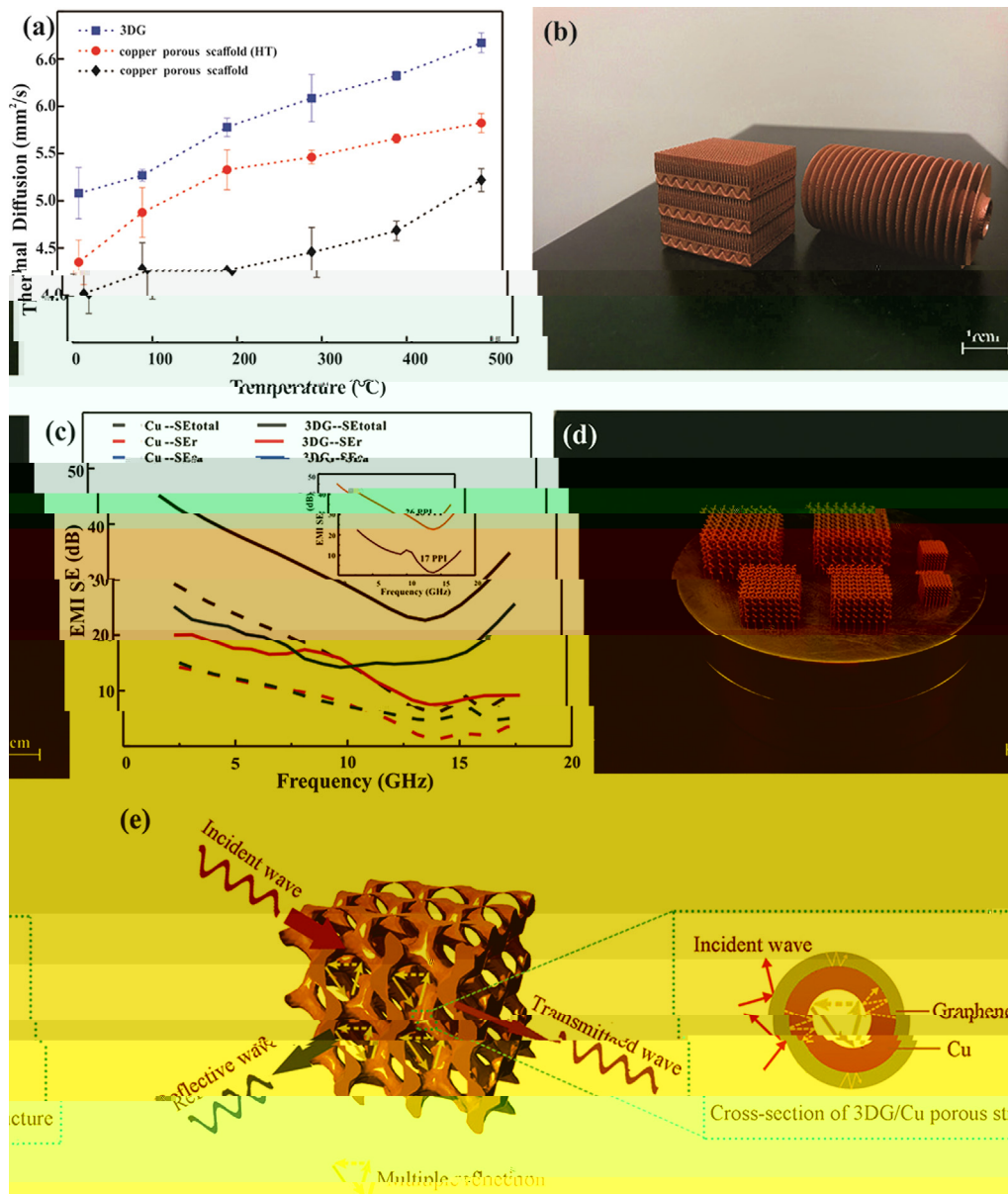


Fig. 9. P 3DG/C ff ; () ff ; () SLM ff fl (3DG/C fl EMI. (F

Table 1

Coating materials	Substrate	Method	Maximum shielding efficiency (dB)	Improvement of thermal property (%)	Ref
G	G	I + + ↓ + ↓	37	-	50
G	PS	H - ↓ + ↓ + ↓ ↓	29.3	-	56
G	PMMA	S ↓ + ↓ +	19	-	57
C /G	/C	A ↓ S fi + ↓ ↓ ↓	-	8.5	58
G	N	F + CVD	-	554	59
G	C -N	H ↓ + ↓ + ↓	20	-	60
G	C	P + CVD	-	2.4	61
G	C	F - + ↓ ↓	47	6.3	62
G	C	CVD + SLM	47.8	27	T

Note: ↓ (↓ ↓)-PPMA, ↓ -PS.

HT
in-situ (F . 9a). S
 3DG/C
 ff
 HT
 1-2
 . I
 fl
 500 μ)
 (F . 9b),
 . G
 (T ↓ 1). I
 N
 T
 EMI, EMI SE,
 (EM)
 2-18 GH (F . 9c),
 ff
 SE
 47.8 B (88.2%)
 3DG/C
 . J K
 133%
 R J V K 45
 . W
 17 26 PPI (F . 9c insert)
 EMI SE. I
 ff
 3DG/C
 32.3 B,
 (30
 3DG/C
 3D
 T
 (SE_a)
 48 . R
 49
 T
 50 . R
 C 51 . F
 52 S O₂ 53 . W

SE_r SE_a
 fi
 F . 9e. W
 3DG/C
 ff
 fl
 3DG/C
 fi
 EM
 fi
 EM
 SE_r. O
 ff
 ff
 J
 54 . I
 fl
 ff . M
 EM
 EM
 . T
 44 . T
 3D
 EM
 CVD
 . I
 R
 S 3.3
 EM
 55 . I
 . O
 3DG/C
 ff
 . T

4. Conclusions

A 3DG/C
in-situ
 ff
 CVD
 ff
 . W
 3DG/C
 EMI SE
 15.9 (
) 32.3 B,
 47.8 B (88.2%)
),
 26.8%
 ff . T
 3DG/C
 fl
 . T
 J
 3DG/C
 EMI
 ff

Credit authorship contribution statement

Kaka Cheng: C
Wei Xiong: V
Yan Li: W &
Liang Hao: F
Zhaoqing Li: V
Yushen Wang: I
Li Lee: D
Ton Peijs: W &
Chunze Yan:
Zhufeng Liu:
Khamis Essa:
Xin Gong: S

Declaration of Competing Interest

T ↓ fl

Acknowledgement

T ↓ N ↓ S ↓ F ↓ C ↓ (N . 51671091, N . 51902295, N . 51675496). T ↓ N ↓ F ↓ R ↓ F ↓ C ↓ U ↓ , C ↓ U ↓ G ↓ (W) (N . (N . CUG170677) H ↓ P ↓ N ↓ S ↓ F ↓ (N . 2019 CFB264).

Appendix A. Supplementary data

S ↓ /10.1016/J . 2020.105904. //

References

1 B RG, N N, M K, M S. G : ↓ ↓
 2 B ↓ AA, G S, B W, C ↓ L, T ↓ D, M F, ↓ S
 3 L ↓ , H, C M, P ↓ H, P ↓ O, S ↓ L ↓ G, ↓ I ↓
 4 K M, K J, J B, C ↓ , K ↓ JH, A ↓ JH. G ↓ ACS A ↓ M ↓ I ↓ 2016;8(36):24112–22.
 5 P ↓ , C M, H M, T M, ↓ L ↓ D. P ↓ ACS N ↓ 2017;11(8):7950–7.
 6 A ↓ C ↓ B 2020;262:118266–76.
 7 L ↓ J ↓ W, C LL, J SH, W ↓ G, ↓ L ↓ C-G ↓ P ↓ A ↓
 2017;101:50–8.
 8 HQ, L SW, C LH, J SH, H HQ. S ↓ J M ↓ C ↓ A ↓
 2018;6(42):21216–24.
 9 D ↓ TM, S ↓ P, D ↓ P, K ↓ J, K ↓ M, A ↓ T, ↓ 3D ↓
 2017;1(4):467–70.
 10 Q ↓ L, L L. T ↓ RSC A ↓ 2014;4(72):38273–80.
 11 D ↓ H ↓ L SP, ↓ N, W ↓ JG. 3D ↓ M S₂ ↓ : P ↓
 2016;90:424–32.
 12 L L, ↓ W, S ↓ CO, H MK, ↓ HL, D ↓ W, ↓ S ↓ - ↓ - ↓
 201803938. ↓ A ↓ F ↓ M ↓ 2018. // ↓ /10.1002/ ↓
 13 L J, P ↓ , C, R ↓ G, ↓ N ↓ D, ↓ G ↓ ACS N ↓
 2013;7(7):6001–6.
 14 J ↓ SH, A ↓ S, G ↓ A. L ↓ - ↓
 2017;56:15520–38.
 15 I ↓ , T ↓ , S ↓ K, K ↓ M, T ↓ T, T ↓ K, ↓ T ↓
 PCCP 2018;20(9):6024–33.
 16 S ↓ K, D ↓ N, M ↓ W, C, V ↓ N, E ↓ J. T ↓
 2002;149(8):370–7.
 17 C ↓ H, S ↓ M, S ↓ WH, L ↓ G, H ↓ Q ↓ , S ↓ 2011;7(22):3163–8.
 18 K ↓ H, G ↓ M, J ↓ I, H ↓ J, W ↓ C, C ↓ M. U ↓
 2019;1(4):1077–87.
 19 S ↓ Q ↓ F ↓ L ↓ W, L ↓ H, L ↓ , ↓ C ↓
 2017;29(31):1701583–90.
 20 ↓ G ↓ C ↓ L, T ↓ H, ↓ D, W ↓ , ↓ T ↓
 ACS N ↓ 2019. // ↓ /10.1021/ ↓ .9 08191.
 21 C ↓ C, H ↓ , B ↓ N ↓ J, C ↓ S, L ↓ F, ↓ 3D ↓ T 6A 4V ↓ :
 ff ↓ M ↓ D ↓ 2019;175:107824–33.
 22 S ↓ š ↓ J, B ↓ ž ↓ D. T ↓ ff ↓ N ↓ B ↓ 316L ↓ SLM. S ↓ C ↓
 T ↓ 2016;307:407–17.

22 R DC, ↓ HB, L ↓ J, L SJ, J ↓ W, ↓ R, ↓ M ↓ . M S E A-S ↓
 2020;771:138586–95.
 23 L ↓ , C ↓ W, A ↓ J, K ↓ S, N ↓ J, ↓ D, ↓ L ↓ - ↓
 2009;324(5932):1312–4.
 24 C ↓ P, R ↓ WC, G ↓ LB, L ↓ BL, P ↓ SE, C ↓ HM. T ↓ - ↓ fl ↓
 2011;10:424–8.
 25 J ↓ SD, D ↓ S, G ↓ L, K ↓ JP, H ↓ JV, V ↓ K ↓
 I fl ↓ J M ↓ P ↓ T ↓ 2019;270:47–58.
 26 W, H ↓ L, L ↓ , T ↓ D, C ↓ Q, F ↓ , ↓ Eff ↓ ↓ ↓ ↓
 2019;170:107697–708.
 27 G ↓ DD, M ↓ W, W ↓ K, P ↓ R. L ↓ . I M R ↓
 2013;57(3):133–64.
 28 L ↓ E, T ↓ S, C ↓ L, F ↓ A. Eff ↓ ↓ ↓ ↓ (SLM) ↓
 316L ↓
 29 ↓ , ↓ J M ↓ P ↓ T ↓ 2017;249:255–63.
 ↓ , ↓ S, W ↓ , L ↓ J, W ↓ P, C ↓ , ↓ F ↓ T 6A 4V. A ↓ P ↓ A: M ↓ S ↓
 P ↓ 2018;124:685–98.
 30 L ↓ , ↓ M ↓ S, D ↓ W, S ↓ C. I ↓ A S 316L ↓ . M ↓ D ↓
 2015;87:797–806.
 31 L ↓ CLA, M ↓ S, T ↓ M, A ↓ RC, W ↓ PJ, L ↓ PD. T ↓ ff ↓ A ↓ M ↓
 2019;166:294–305.
 32 T ↓ , K ↓ , T ↓ WQ, T ↓ J, D ↓ M, M ↓ ↓ D, ↓ R ↓ - ↓
 α/β
 T-6A-4V. S R 2016;6:26039–48.
 33 K ↓ H, T ↓ P, L ↓ NH, T ↓ SB, C ↓ CK. G ↓ - ↓ T-6A-4V ↓ . V ↓
 P ↓ P ↓ 2016;11(3):183–91.
 34 R fi HK, K ↓ NV, G ↓ H, S ↓ TL, S ↓ BE, M ↓
 6 ↓ 4 ↓
 2013;22(12):3872–83.
 35 T ↓ , K ↓ , T ↓ J, V ↓ G, P ↓ Q ↓ , ↓ G ↓ . A ↓ ↓ ↓
 T-6A-4V. J A ↓ C ↓ 2015;646:303–9.
 36 R ↓ DA, M ↓ LE, M ↓ H ↓ , ↓ N ↓ - ↓
 ↓ A ↓ M ↓ 2011;59(10):4088–99.
 37 ↓ , ↓ , ↓ W ↓ H. Eff ↓ C ↓ 2.4N-0.7S ↓ . J A ↓ C ↓
 2018;743:258–61.
 38 K ↓ S. W ↓ W ↓ . S ↓ E ↓ 2003;23:309–48.
 39 L ↓ G ↓ , G ↓ J ff ↓ R, G ↓ N ↓ P. E ↓ C (111). N ↓
 L ↓ 2010;10(9):3512–6.
 40 L ↓ S, C ↓ WW, C ↓ L ↓ R ↓ ffR ↓ S. E ↓ N ↓
 C ↓ N ↓ 2009;9(12):4268–72.
 41 ↓ W, ↓ C, ↓ W ↓ H, ↓ SQ ↓ L. A ↓ . C ↓
 2020;161:479–85.
 42 F ↓ AC, M ↓ JC, S ↓ V, C ↓ C, L ↓ M, M ↓ F, ↓ R ↓
 2006;97(18):187401–4.
 43 ↓ S ↓ , ↓ G ↓ J ↓ SH, F ↓ PC, H ↓ HQ. H ↓ ↓ ↓ ↓
 M ↓ L ↓ 2017;200:97–100.
 44 J ↓ K ↓ H, ↓ J, C ↓ J, D ↓ . F ↓ C ↓ -N ↓ CNT ↓
 A ↓ S ↓ S ↓ 2014;311:351–6.
 45 R ↓ J ↓ K, M ↓ DP, A ↓ C, M ↓ S, S ↓ MK. E ↓ EMI ↓ ↓ ↓
 . C ↓ P ↓ A ↓ 2018;12:475–84.
 46 S ↓ B, L ↓ , ↓ W, ↓ W. C ↓ (EMI) ↓ . ACS ↓
 A ↓ M ↓ I ↓ 2016;8(12):8050–7.
 47 L ↓ N, H ↓ , D ↓ F, H ↓ , L ↓ , G ↓ 6 66;97141;161:479

53 M 2019;34(5):489–98.
W B, C M, L M. R . A M

54 C H, W S, J , J, C J, S ff F₃O₄
2014;26:3484–9.
2019;121:139–48.
W L, J, Q. T ff MWCNT . J M S : M B
-MWCNT

56 D , P GR, H P, Q F, M B , ML. Effi . J. M
2015;26(3):1895–9.

57 C 2012;22:18772–4.
HB, Q, WG, H , T . ACS A M I

58 S A, U N, T V. T
2011;3:918–24.
M R 2016. :// . /10.1051/ /2016021.

59 P MT, J H, R ff RS, S L. T . N L
2012;12:2959–64.

60 J K, H, H , D . P C -N M L
2017;122:244–7.

61 R H, L S, B S, K TW, L DS, L HJ, T
. S R 2015. :// . /10.1038/ 12710.
T, F SG, L , G Q, L G, R KP, S

62 . M S E A-S 2020. :// . /10.1016/J
.2019.105670.

63 R DA, M LE, M E, H DH, M JL, M BI, . A
N

64 M 2011;59(10):4088–99.
E SF, L KC, S VK, M IC. T . J T
E 1973;1(1):10–38.